Susceptibility of Cyclin-dependent Kinase Inhibitor-1−deficient Mice to Rheumatoid Arthritis From IL-1β−induced Inflammation

Yoshinori Takashima
Kobe University Graduate School of Medicine

Shinya Hayashi (✉ s11793290@yahoo.co.jp)
Department of Orthopaedic Surgery, Kobe University Graduate School of Medicine, 7-5-2, Kusunoki-chou, Chuo-ku, Kobe 650-0017, Hyogo, Japan

Koji Fukuda
Kobe University Graduate School of Medicine

Toshihisa Maeda
Kobe University Graduate School of Medicine

Masanori Tsubosaka
Kobe University Graduate School of Medicine

Tomoyuki Kamenaga
Kobe University Graduate School of Medicin

Kenichi Kikuchi
Kobe University Graduate School of Medicin

Masahiro Fujita
Kobe University Graduate School of Medicin

Yuichi Kuroda
Kobe University Graduate School of Medicine

Shingo Hashimoto
Kobe University Graduate School of Medicine

Naoki Nakano
Kobe University Graduate School of Medicine

Tomoyuki Matsumoto
Kobe University Graduate School of Medicine

Ryosuke Kuroda
Kobe University Graduate School of Medicine

Research article

Abstract

Background: Rheumatoid arthritis (RA) is a chronic and systemic inflammatory disorder whose progression is modulated by fibroblast-like synoviocytes (FLSs). Cyclin-dependent kinase (CDK) inhibitor 1 (p21) regulates the activation of other CDKs, and we recently reported that p21 deficiency induces susceptibility to osteoarthritis. Here, we focused on joint inflammation to determine the mechanisms associated with p21 function in synovial and cartilage tissues in RA.

Methods: p21-knockout (p21$^{-/-}$) mice and wild-type C57BL/6 (WT p21$^{+/+}$) mice were used to establish a collagen antibody-induced arthritis (CAIA) model. The severity of arthritis was evaluated visually, and histological and immunohistological analyses performed 7, 14, and 28 days after injection with a cocktail of five monoclonal antibodies that recognize conserved epitopes on various species of type II collagen. The response of p21 siRNA-treated human RA FLSs to IL-1β stimulation was also determined.

Results: Arthritis scores were higher in p21$^{-/-}$ mice than those in p21$^{+/+}$ mice. More severe and prolonged synovitis of the knee joints and earlier loss of staining and cartilage destruction were observed in p21$^{-/-}$ mice than in p21$^{+/+}$ mice. p21$^{-/-}$ mice expressed higher levels of IL-1β, F4/80, p-IKKα/β, and MMPs in cartilage and synovial tissues at each time point, except for before injection of the monoclonal antibodies, via IL-1β-induced NF-kB signaling. IL-1β stimulation significantly increased MMP expression and enhanced IKKα/β phosphorylation in human FLSs.

Conclusion: p21-deficient CAIA mice are susceptible to alterations in the RA phenotype, including joint cartilage destruction and severe synovitis, via IL-1β-induced inflammation. Therefore, p21 regulation may constitute a possible strategy for RA treatment.

Background

Rheumatoid arthritis (RA) is characterized by chronic synovial inflammation of multiple joints (1, 2). The affected synovial tissues contain activated macrophages, fibroblasts, and T and B lymphocytes that are induced by pro-inflammatory cytokines, such as interleukin (IL)-1β, tumor necrosis factor-α (TNF-α), and IL-6. The cytokines provoke and perpetuate the synovial membrane inflammation in the joints, which leads to articular cartilage damage and bone erosion (3, 4). Especially, activated RA fibroblast-like synoviocytes (FLSs) contribute to the inflammatory and destructive potential of the aggressive pannus tissue in patients with RA by producing pro-inflammatory mediators and matrix metalloproteinases (MMPs), such as MMP-1, MMP-3, and MMP-9 (5-11). Moreover, IL-1β, which is produced by chondrocytes, osteoblasts, mononuclear cells, and cells forming synovial membranes, is secreted into the hip and knee joints during an inflammatory response (12). IL-1β affects the synthesis of MMPs, specifically MMP-13, in the chondrocytes, resulting in cartilage destruction (13). Patients with RA display elevated IL-1β levels in FLSs, the synovial fluid, the synovial membrane, cartilage, and the subchondral bone layer (6), suggesting that IL-1β may be involved in the pathogenesis and progression of RA.

Animal models of RA, including collagen rat and mouse models of type II-induced arthritis, rat model of adjuvant-induced arthritis, and models of antigen-induced arthritis in several species, have proven to be highly predictive of therapeutic efficacy in humans (14). In particular, the collagen antibody-induced arthritis (CAIA) model mouse is ideal for rapid screening of novel arthritis therapeutics and elucidating the mechanisms involved in the development of arthritis (15). In this model, arthritis is induced through systemic administration of antibody mixtures that target various epitopes of type II collagen. Moreover, this method can induce arthritis in various mouse strains, not just CAIA-susceptible mice, making it ideal for studying the pathological role of individual gene products, such as cytokines, without the influence of complete or incomplete Freund's adjuvant that may strongly affect the host immune system.

 Cyclin-dependent kinase inhibitor 1 (p21) was initially identified as a potent inhibitor of cell-cycle progression (16-19). Its knockout induces a regenerative response in an appendage of an otherwise non-regenerating mouse strain (20). It has been shown to regulate cell proliferation and inflammation after arterial injury in local vascular cells (21). Subsequent studies have also identified the importance of p21 in controlling inflammation, cytostasis, and cell death (22). Transcription of p21, which is activated by the tumor suppressor protein p53, is part of a negative-feedback mechanism that controls p53 activity during apoptosis (23). $p21^{-/-}$ mice have been shown to lack any overt skeletal phenotype and are unlikely to develop spontaneous malignancies (24-26).

We recently reported that p21 deficiency induces susceptibility to osteoarthritis (OA) through signal transducer and activator of transcription 3 (STAT3)- and IL-1β-induced activation of nuclear factor kappa-light-chain-enhancer of activated B cells (NF-κB) signaling (27, 28). Recent studies have also shown that p21 plays a key role in suppressing activated macrophages (29), and that expression of *p21* in rheumatoid synovial fibroblasts resulted in downregulation of inflammatory mediators and tissue-degrading proteinases in RA (30).While the expression of p21 is decreased in RA FLSs (31), it is unclear how p21 affects the joint synovial tissues and cartilage in RA.

In this study, we hypothesized that p21 deficiency enhances joint inflammation and cartilage destruction in RA. We evaluated the degree of joint inflammation to determine the mechanisms associated with p21 function *in vitro* as well as *in vivo* using RAFLS and the systemic arthritis model, respectively.

Methods

Generation of homozygous $p21^{-/-}$ mice

Homozygous B6.129S6 (Cg)-Cdkn1atm1 Led/J mice were obtained from the Jackson Laboratory (Bar Harbor, ME, USA). We backcrossed these mice for ten generations against a C57BL/6 background, obtained from CREA Japan, Inc (Tokyo, Japan), and studied 10-week-old male mice (n=16). $p21^{+/+}$ littermates were used as WT controls (n=16). Genotyping was performed using PCR-based amplification of mouse-tail DNA with allele-specific probes. Both the $p21^{+/+}$ and $p21^{-/-}$ groups contained four mice. All animals were bred in a mouse house with automatically controlled lighting (12 h light/dark cycle) and a

stable temperature of 23 °C and were allowed *ad libitum* access to food and water throughout the study. This study was performed in strict accordance with the recommendations of the Guide for the Care and Use of Laboratory Animals published by the National Institutes of Health (Bethesda, MD, USA). All procedures were approved by the Animal Studies Committee of Kobe University, Japan (permit number: P180404).

Establishment of a CAIA mouse model

A cocktail of five monoclonal antibodies recognizing the conserved epitopes on various species of type II collagen (Chondrex Inc., Redmond, WA, USA) was prepared as described previously (2) and used according to the manufacturer's instructions. Mice were injected with the cocktail of antibodies intraperitoneally (i.p.; 5 mg). Three days later, they were injected with 50 μg lipopolysaccharide (LPS) from *Escherichia coli* 0111: B4 (Chondrex Inc.) i.p. to induce arthritis. On days 7, 14, and 28 (counting from day 0 as the day of cocktail injection), at least four mice each from the p21$^{-/-}$ and WT groups were euthanized using CO_2. We defined the mice without injection of monoclonal antibodies as the control mice.

Evaluation of arthritis

The mice were blindly evaluated for disease progression on days 0, 3, 7, 10, 14, and 28. The severity of arthritis in each paw was graded on a scale of 0–4, as follows: 0, normal; 1, mild swelling; 2, moderate swelling; 3, severe swelling; 4, pronounced edema of the entire paw. The cumulative score from all four paws (maximum score of 16 per mouse) was used as the overall disease score (32).

Histological evaluation for cartilage degeneration and synovitis

Mouse knee joints were fixed using 4% paraformaldehyde (163-20415, WAKO, Osaka, Japan) for 24 h, decalcified with 14% ethylenediaminetetraacetic acid (EDTA; 345-01865, Dojindo, Kumamoto, Japan) for 7 d, and embedded in paraffin. Histological coronal sections were obtained from the joint at 80-μm intervals and stained with Safranin-O (S0145, Tokyo Chemical Industry, Tokyo, Japan) and Fast Green (10720, Chroma-Gesellschaft, Thermo Fisher Scientific, Inc). RA histopathology was evaluated using the Osteoarthritis Research Society International (OARSI) cartilage OA-histopathology scoring system. Histological scores were measured in the four quadrants (i.e., medial femoral condyle, medial tibial plateau, lateral femoral condyle, and lateral tibial plateau) of the knee joints at all sectioned levels (eight sections per knee) to obtain summed scores. The summed scores were calculated from all four quadrants of all sections that represented whole-joint changes (33). Synovitis was also evaluated using the OARSI-recommended scoring system of hematoxylin-eosin-stained sections (34). Two specimens from each compartment were evaluated and the highest score was recorded. The average of each compartment score was considered as the whole-knee score.

Immunohistochemistry

Deparaffinized sections were digested with proteinase (Dako, Glostrup, Denmark) for 10 min and treated with 3% hydrogen peroxide (Wako Pure Chemical Industries, Osaka, Japan) to block endogenous peroxidase activity. We assessed F4/80 expression—using a previously reported scoring system for immunohistochemistry—as an immune and inflammatory cell marker because it is a well-known macrophage marker (35).

The sections were probed with the following antibodies (1:50 dilution) at 4 °C overnight: anti-F4/80 (MCA497P647T, AbDSerotec, Kidlington, UK), anti-IL-1β (ab9722, Abcam), phosphor-IκB kinase complex (IKK) α/β (#2697S, Cell Signaling Technology, Danvers, MA, USA), anti-MMP-3 (SC-21732, Santa Cruz Biotechnology, Dallas, TX, USA), anti-MMP-13 (ab39012, Abcam), or anti-MMP-9 (10375-2-AP, Proteintech Group, Chicago, IL, USA). Sections were subsequently probed with peroxidase-labeled anti-rabbit or rat IgG (Histofine Simple Stain MAX PO; Nichirei Bioscience, Tokyo, Japan) antibody at 23–27 °C for 1 h. The brown reaction product was generated as a signal upon addition of the peroxidase substrate 3,3'-diaminobenzidine (Histofine Simple Stain DAB solution; Nichirei Bioscience), and the sections were examined under an optical microscope. Hematoxylin was used as a counterstain.

 One coronal section from the center of the most severe lesion in each tibial plateau was scored. The numbers of stained cells were counted in three areas of high-magnification fields at both superficial and deep zones of the cartilage tissue by triple-blinded observers. The average percentages of MMP-3-, MMP-13-, p-IKKα/β-and IL-1β-positive cells/total cells were calculated. Each coronal section from each of the four mice was evaluated for each group. The positive cells were included superior of the tidemark.

Preparation of human synovium

Synovial tissues were obtained during a total knee joint replacement surgery from five patients with RA. All RA patients fulfilled the American College of Rheumatology 1987 revised criteria for RA (36). OA synovial tissues were also obtained during total knee joint replacement surgery from five patients, as controls. Diagnoses of OA were based on clinical, laboratory, and radiographic evaluations. All samples were obtained in accordance with the World Medical Association Declaration of Helsinki Ethical Principles for Medical Research Involving Human Subjects. The study protocol was approved by the Kobe University Graduate School of Medicine Ethics Committee, and all participants provided informed consent.

Preparation of cell culture

Primary synoviocytes were isolated and cultured from the RA and OA synovial tissues. The tissues were minced and incubated with trypsin (0.5 mg/ml; Sigma-Aldrich, St. Louis, MO, USA) for 15 min at 37 °C, after which the synovium was treated with Dulbecco's modified Eagle's medium (DMEM; Gibco/Life Technologies, Grand Island, NY, USA) containing 0.2% collagenase (Sigma-Aldrich) at 37 °C for 15 h. Dissociated cells were cultured overnight in DMEM supplemented with 10% fetal bovine serum (BioWhittaker FBS; Lonza, Walkersville, MD, USA) and 100 U/ml penicillin-streptomycin. The non-adherent

cells were removed, and the adherent cells were further incubated on a 6-well plate with fresh medium (3×10^5 cells/well). All experiments were conducted using 3–5 passage cells.

Transfection of small-interfering RNA

Lipofectamine^{TM} RNAiMax transfection reagent (Invitrogen) was used to transfect p21 small-interfering RNA (siRNA) and nonspecific siRNA control into the RA and OA human knee synoviocytes, respectively, according to the manufacturer's recommendations. Briefly, a day before transfection, the cells (3×10^5 cells/well) were seeded in a 6-well plate with growth medium without antibiotics to achieve 30–50 % confluence at the time of transfection. Subsequently, 5 pmol of siRNA and Lipofectamine^{TM} RNAiMax complexes were prepared and added to each well. After transfection for 24 h, the complexes were removed and fresh medium containing 10% FBS was added.

Quantitative reverse transcriptase-polymerase chain reaction (RT-PCR)

Cultured RA and OA synoviocytes were transfected with the p21 siRNA or nonspecific siRNA control. FLSs without siRNA transfection were used as controls. After transfection for 24 h, the cells were incubated for another 24 h with or without stimulation with 10 ng/ml recombinant human IL-1β(R&D systems, McKinnley, MN, USA), followed by RNA extraction using a QIA shredder and RNeasy Mini Kit (Qiagen, Hilden, Germany) according to the manufacturer's protocol. Briefly, 1 μg of total RNA was reverse-transcribed to first-strand cDNA using 1.25 μM oligo-dT primer in 40 μl PCR buffer II containing 2.5 mM MgC1$_2$, 0.5 mM dNTP mix, 0.5 U of RNase inhibitor, and 1.25 U of murine leukemia virus reverse transcriptase (PerkinElmer/Applied Biosystems, Foster City, CA, USA), at 42 °C for 1 h. The relative expression levels of mRNA encoding human p21, MMP-3, and MMP-9 were analyzed using SYBR Green RT-PCR on an ABI Prism 7500 sequence detection system (Applied Biosystems, Foster City, CA, USA). Relative gene expression was normalized against the GAPDH housekeeping gene using the comparative cycle threshold (Ct) method. The difference between the mean Ct values of the gene of interest and those of the housekeeping gene is denoted as ΔCt, whereas the difference between the ΔCt and the Ct value of the calibrator sample is denoted as ΔΔCt. The $\log_2$ (ΔΔCt) value gives the relative level of gene expression. The primer sequences used for the detection of human p21, MMP-3, and MMP-9 are listed in Supplementary Table 1.

Western blot analysis

First, the cultured RA synoviocytes were treated with or without 10 ng/ml recombinant human IL-1β (R&D Systems) for 5, 10,15, 30, and 60 min; stimulation time for IL-1β was determined as previously reported (37). The synoviocytes were washed with Tris-buffered saline with Tween-20 (TBST) and lysed in a buffer containing 25 mM Tris, 1% Nonidet P-40, 150 mM NaCl, 1.5 mM ethylene glycol tetraacetic acid, and a protease/phosphatase inhibitor mix (Roche Diagnostics, Basel, Switzerland). The lysates were centrifuged at 4 °C at 15,000 × g for 10 min to remove cellular debris. Next, the cellular debris-free lysates were collected and mixed with 4× electrophoresis sample buffer; 15 μl of cell lysates (1.0×10^7 cells/ml)

were electrophoresed on a 7.5–15% SDS-polyacrylamide gradient gel (Biocraft, Tokyo, Japan) and electrically transferred onto a polyvinylidene difluoride blotting membrane (GE Healthcare Life Sciences, Little Chalfont, UK). The membrane was blocked with 5% skimmed milk in TBST at 25 °C for 30 min, incubated with antibodies against anti-p-IKKα/β (Cell Signaling Technology) at 4 °C for 12 h, and further incubated with horseradish peroxidase-conjugated goat anti-rabbit IgG secondary antibody at 25 °C for 1 h. The proteins were subsequently visualized using ECL Plus reagent (GE Healthcare Life Sciences) in a chemilumino analyzer (LAS-3000 mini; Fujifilm, Tokyo, Japan).

The cultured RA and OA synoviocytes were then transfected with p21 siRNA or nonspecific siRNA control. After 24 h of transfection, the cells were incubated with or without IL-1β stimulation for the period with the highest level of p-IKKα/β in the western blot. Western blots of the synoviocytes were subsequently subjected to the same procedure as described above. Expression of the alpha-tubulin protein was detected using rabbit anti-alpha-tubulin polyclonal antibody (catalog no. ab4074; Abcam) as a primary antibody. Protein expression was determined semi-quantitatively with the National Institutes of Health ImageJ software (http://imagej.nih.gov/ij/) using digitally captured images. Five different samples were analyzed for each experiment.

Statistical analysis

Statistical analysis was performed using one-way (Figures 5B and 6A) or two-way (Figures 1A, 1C, 1E, 2B, 3B, 3D 4B, 4E, 5C, 5D, and 6B) analysis of variance and Tukey's post hoc test for multiple comparisons of paired samples. The Mann-Whitney U test was used for comparisons between two groups (Figure 5A). Results are presented as means with 95% confidence intervals and were considered statistically significant at $P < 0.05$.

Results

p21-deficient mice are susceptible to joint destruction *in vivo*

Severe arthritis was observed in p21$^{-/-}$ mice after injection of the monoclonal antibody cocktail. The arthritis scores on days 7, 10, 14, and 28 of p21$^{-/-}$ mice were significantly higher than those of p 21$^{+/+}$ mice at each time point (Figure 1A). Based on Safranin-O and Fast Green staining, p21$^{-/-}$ mice showed an earlier loss of Safranin-O staining than both the control and p21$^{+/+}$ mice on day 7 (Figure 1B). Both p21$^{-/-}$ and p21$^{+/+}$groups showed loss of Safranin-O staining, but the articular surface layer remained intact on day 14 (Figure 1B). While p21$^{-/-}$ mice showed mid-zone excavation of cartilage tissue, the articular surface of p21$^{+/+}$ mice remained intact on day 28 (Figure 1B). According to the OARSI cartilage OA-histopathology scoring system, the average sum score of p21$^{-/-}$ mice increased significantly compared with that of p21$^{+/+}$ mice on day 28 (Figure 1C).

p21-deficient mice are susceptible to severe synovitis

Histological analysis using hematoxylin-eosin staining showed that synovitis of the knee joints was more severe and more prolonged in p21$^{-/-}$ mice than in p21$^{+/+}$ mice (Figure 1D). On days 7 and 14, p21$^{-/-}$ mice showed marked cellular infiltration mixed with lymphoid follicles, multiple-layered synovial lining cells, and villous hyperplasia compared with the control (Figure 1D). Moreover, on day 28, p21$^{-/-}$ mice displayed prolonged synovitis, whereas synovitis was attenuated in p21$^{+/+}$ mice at this time point (Figure 1D). According to the OARSI synovitis-severity scoring system, more severe synovitis was observed in p21$^{-/-}$ mice than in p21$^{+/+}$ mice at all time points (Figure 1D, E). There was no significant difference in synovitis severity of p21$^{-/-}$ mice between days 7 and 14 (Figure 1D, E).

p21-deficient mice exhibited enhanced inflammatory cytokine expression

p21$^{-/-}$ mice showed higher IL-1β expression in cartilage tissues compared with p21$^{+/+}$ mice at each time point except for the control (Figure 2A). IL-1β expression in synovial tissues was also increased in p21$^{-/-}$ mice compared with the p21$^{+/+}$ mice at each time point except for the control (Figure 2C). The IL-1β-positive-cell ratio in the cartilage was significantly higher in p21$^{-/-}$ mice than in p21$^{+/+}$ mice at each time point except for the control (Figure 2B), and those of IL-1β on day 7 and thereafter were significantly higher than those of the control (Figure 2B). There was no significant difference in the positive-cell ratio of p21$^{-/-}$ mice between days 7 and 14 (Figure 2A, B). Moreover, the expression of IL-1β in p21$^{-/-}$ peaked on days 7 and 14 and was delayed compared with the peak IL-1β in p21$^{+/+}$ mice (Figure 2A, B).

p21 deficient mice exhibited enhanced macrophage infiltration and increased expression of inflammatory transcription factors in synovial tissues

F4/80-expression levels were elevated in the synovial tissue of p21$^{-/-}$ mice at each time point except the control, indicating increased macrophage infiltration (Figure 3A). The F4/80 score was significantly higher in p21$^{-/-}$ mice than in p21$^{+/+}$ mice at each time point except for the control (Figure 3A, B). On day 7 and thereafter, the F4/80 score was significantly higher in p21$^{-/-}$ mice than in controls (Figure 3B). Moreover, F4/80 expression in p21$^{-/-}$ mice peaked on day 14, which was delayed compared with that in p21$^{+/+}$ mice (Figure 3A, B). p21$^{-/-}$ mice showed higher p-IKKα/β expression in the cartilage and synovial tissues compared with p21$^{+/+}$ mice at each time point except for the control (Figure 3C, E). The positive-cell ratio of p-IKKα/β in the cartilage was significantly higher in p21$^{-/-}$ mice than in p21$^{+/+}$ mice at each time point except for control (Figure 3C, D), and the ratios of p-IKKα/β in p21$^{-/-}$ mice on day 7 and thereafter were significantly higher than those in the control (Figure 3D). There was no significant difference in the positive-cell ratio of p21$^{-/-}$ mice between day 7 and day 14 (Figure 3B–D). Moreover, the expression of p-IKKα/β in p21$^{-/-}$ peaked on day 14, which was delayed compared with that in p21$^{+/+}$ mice (Figure 3D).

p21-deficient mice exhibited joint destruction through elevated MMPs expression

MMP-3 and MMP-9 expression levels were elevated in the synovial tissues of p21$^{-/-}$ mice at each time point except for the control (Figure 4C and Supplementary Figure 1A). The positive-cell ratios of MMP-3 and MMP-13 in the cartilage were significantly higher in p21$^{-/-}$mice than in p21$^{+/+}$ mice at each time point except for the control (Figure 4A, D), and positive-cell ratios of MMP-3 and MMP-13 on day 7 and thereafter were significantly higher than those of the control (Figure 4B, E).

Downregulation of p21 gene expression enhanced MMPs expression through IL-β stimulation in RA synovial tissues

RT-PCR analysis showed that expression levels of p21 were lower in human RAFLS than OA FLS and that MMP3 and MMP9 were highly expressed in RA FLS (Figure 5A). Expression of the p21 gene was inhibited by 14.7% and 18.6% in RA FLS and OA FLS, respectively, after transfection with p21-specific siRNA (Figure 5B). MMP3 expression was increased by 157-fold and 26-fold in p21 knockdown RA FLS and OA FLS, respectively, through IL-β stimulation (Figure 5C), whereas MMP9 expression was increased by 3.7-fold and 3.4-fold in p21 knockdown RA FLS and OA FLS, respectively (Figure 5D).

Downregulation of p21 gene expression enhanced phosphorylation of IKKα/β in RA synovial tissues

Western blot demonstrated that the expression of phosphorylated IKKα/β (p-IKKα/β) markedly increased after a 15 min treatment with 10 ng/ml IL-1β (Figure 6A). Therefore, the RA FLS and OA FLS were treated with IL-1β for 15 min in subsequent experiments. The downregulation of p21 gene expression enhanced the phosphorylation of IKKα/β in RA FLS compared with that in OA FLS (Figure 6B).

Discussion

In this study, we demonstrated that p21-deficient mice presented enhanced cartilage degradation and more severe synovitis in response to systemic inflammation through NF-κB signaling in cartilage and synovial tissues.

Similar to our study, previous reports have shown increased arthritis scores and observed histological changes, including a marked increase in cellular infiltration, in the knee synovial membrane of p21$^{+/+}$ CAIA mice (38). Moreover, we found severe arthritis in p21$^{-/-}$mice than in p21$^{+/+}$ mice on day 7 and thereafter, suggesting that downregulation of p21 may exacerbate CAIA and enhance macrophage infiltration in mice. IL-1β expression in p21$^{-/-}$ mice reportedly increased 2.4-fold compared to that in p21$^{+/+}$ mice in an experimental endotoxic shock model *in vivo*, and that in p21$^{-/-}$bone marrow-derived macrophages with LPS stimulation increased 3.4-fold compared to that in p21$^{+/+}$ cells *in vitro* (39). We have previously reported that *p21* knockout in a murine model of destabilization of the medial meniscus increased IL-1β serum levels and local IL-1β expression in knee joints on day 1 and day 56 post-surgery (28). Macrophages play important roles in inflammation, ranging from antigen presentation, phagocytosis, and immunomodulation via the production of various inflammatory cytokines, including IL-1β and TNF-α (39, 40). The importance of macrophages in RA has been shown in several studies,

including the study by Trakala et. al that reported increased IL-1β and TNF-α expression in p21$^{-/-}$ macrophages in an *in vitro* study (41), and by Mavers et al. who found remarkably increased macrophage infiltration in the ankles of a p21$^{-/-}$ arthritis mouse model on days 7, 14, and 25 and significantly elevated IL-1α serum levels on day 7 (29). Our current study also found that p21$^{-/-}$CAIA model mice exhibited prolonged joint arthritis with macrophage infiltration and elevated local IL-1β expression *in vivo*. These findings suggest that macrophages have a critical role in joint inflammation in this mouse model.

Previous reports have shown that IL-1β stimulates NF-κB signaling and induces the expression of MMP-3, MMP-9, and MMP-13 (13, 42), and it is known that the IKK complex plays a central role in the regulation of NF-κB activity (43). In this study, we confirmed that the expression levels of p-IKKα/β, MMP-3, and MMP-13 in chondrocytes and of p-IKKα/β, MMP-3, and MMP-9 in synovial tissues were found to be elevated in p21$^{-/-}$ mice compared with those in p21$^{+/+}$ mice. These findings suggest that rapid joint destruction was caused by elevated levels of inflammation induced via p-IKKα/β signaling. Perlman et al. reported that synovial fibroblasts from p21-deficient mice enhances IL-6 and MMP-3 mRNA levels and cause a 100-fold increase in IL-6 protein levels (31). Hence, alterations in p21 expression may enhance pro-inflammatory cytokine and MMP production, thereby promoting development of autoimmune diseases (31). These earlier studies support our results that p21-deficient mice exhibit enhanced MMP-3, MMP-9, and MMP-13 expression through IL-1β-induced NF-κB signaling.

Consistent with our results, RA FLSs have been shown to exhibit decreased p21 expression (31) and higher IL-1β levels (6, 44) compared with OA FLSs. Moreover, previous studies have demonstrated increased IL-6 and MMP levels in RA FLSs through TNF-α stimulation (45, 46). Consequently, the decline in p21 expression in RA FLSs might cause severe inflammation through IL-1β-induced NF-κB signaling. Furthermore, we have demonstrated that downregulation of p21 in FLSs alters the cellular response to IL-1β stimulation. IL-1β stimulation increased MMP-3 and MMP-9 expression and enhanced p-IKKα/β activation in both RA FLSs and OA FLSs. However, the responses to IL-1β in RA FLSs and OA FLSs were different, indicating that decreased expression of p21 in RA joints may account for the observed joint destruction.

The applicability of the results from this study to human arthritis is limited by the use of an experimental animal model of antibody to collagen-induced arthritis. Clearly, the human scenario is much more complex than can be recreated in the CAIA model. In this study, we showed only the relationship between p21 and IL-1β, but there are many inflammatory pathways associated with RA pathogenesis, for instance, TNF-α and IL-6, among others. Hence, further investigation of these other pathways is needed.

Conclusions

Overall, we demonstrated that p21-deficient CAIA mice were susceptible to joint cartilage destruction and severe synovitis via IL-1β-induced inflammation *in vivo*. We have also shown that downregulation of p21 led to enhanced susceptibility to inflammation through IL-1β stimulation in RA FLSs compared with OA FLSs. Therefore, p21 regulation may constitute a possible therapeutic strategy for RA treatment. However,

given that p21 is an oncogene involved in cell-cycle regulation, further research is required to verify the viability and safety of p21-based therapies for RA treatment.

List Of Abbreviations

RA, rheumatoid arthritis; IL, interleukin; TNF-α, tumor necrosis factor-α; FLSs, fibroblast-like synoviocytes; MMP, matrix metalloproteinases; CAIA, collagen antibody-induced arthritis; p21, cyclin-dependent kinase inhibitor 1; OA, osteoarthritis; NF-κB, nuclear factor kappa-light-chain-enhancer of activated B cells; WT, wild-type; IKK, phosphor-IκB kinase complex.

Declarations

Ethics approval and consent to participate

This study was performed in strict accordance with the recommendations of the Guide for the Care and Use of Laboratory Animals published by the National Institutes of Health (Bethesda, MD, USA). All procedures were approved by the Animal Studies Committee of Kobe University, Japan (permit number: P180404). Synovial tissues were obtained during a total knee joint replacement surgery from five patients with RA and OA. All samples were obtained in accordance with the World Medical Association Declaration of Helsinki Ethical Principles for Medical Research Involving Human Subjects. The study protocol was approved by the Kobe University Graduate School of Medicine Ethics Committee, and all participants provided informed consent.

Consent for publication

Not applicable.

Availability of data and materials

The datasets used and/or analysed during the current study are available from the corresponding author on reasonable request.

Competing interests

All the authors state that they have no conflicts of interest.

Funding

Authors' contributions

YT, KF, and SH made substantial contributions to the design of the study, acquisition, analysis, interpretation of data, and writing of the manuscript. MT, TK, KK and MF participated in the design of the study, acquiring data. TM critically contributed to revising the manuscript enhancing its intellectual content. TM and RK participated in approving the final content of the manuscript. All authors read and approved the final manuscript.

Acknowledgments

References

1. Rooney M, Condell D, Quinlan W, Daly L, Whelan A, Feighery C, et al. Analysis of the histologic variation of synovitis in rheumatoid arthritis. Arthritis Rheum. 1988;31:956-63.

2. Scott DL, Grindulis KA, Struthers GR, Coulton BL, Popert AJ, Bacon PA. Progression of radiological changes in rheumatoid arthritis. Ann Rheum Dis. 1984;43:8-17.

3. Huber LC, Distler O, Tarner I, Gay RE, Gay S, Pap T. Synovial fibroblasts: key players in rheumatoid arthritis [review]. Rheumatology (Oxford). 2006;45:669-75.

4. Lefèvre S, Knedla A, Tennie C, Kampmann A, Wunrau C, Dinser R, et al. Synovial fibroblasts spread rheumatoid arthritis to unaffected joints. Nat Med. 2009;15:1414-20.

5. Brzustewicz E, Bryl E. The role of cytokines in the pathogenesis of rheumatoid arthritis – Practical and potential application of cytokines as biomarkers and targets of personalized therapy. Cytokine. 2015;76:527-36.

6. Dayer JM, Bresnihan B. Targeting interleukin-1 in the treatment of rheumatoid arthritis [review]. Arthritis Rheum. 2002;46:574-8.

7. Lipsky PE, van der Heijde DM, St Clair EW, Furst DE, Breedveld FC, Kalden JR, et al. Infliximab and methotrexate in the treatment of rheumatoid arthritis: anti-tumor necrosis factor trial in rheumatoid arthritis with concomitant therapy study group. N Engl J Med. 2000;343:1594-602.

8. McInnes IB, Schett G. Cytokines in the pathogenesis of rheumatoid arthritis. Nat Rev Immunol. 2007;7:429-42.

9. Murphy G, Nagase H. Progress in matrix metalloproteinase research [review]. Mol Aspects Med. 2008;29:290-308.

10. Vincenti MP, Coon CI, Brinckerhoff CE. Nuclear factor kappaB/p50 activates an element in the distal matrix metalloproteinase 1 promoter in interleukin-1beta-stimulated synovial fibroblasts. Arthritis Rheum. 1998;41:1987-94.

11. Xue M, McKelvey K, Shen K, Minhas N, March L, Park SY, et al. Endogenous MMP-9 and not MMP-2 promotes rheumatoid synovial fibroblast survival, inflammation and cartilage degradation.

Rheumatology (Oxford). 2014;53:2270-9.

12. de Lange-Brokaar BJ, Ioan-Facsinay A, van Osch GJ, Zuurmond AM, Schoones J, Toes RE, et al. Synovial inflammation, immune cells and their cytokines in osteoarthritis: a review. Osteoarthritis Cartilage. 2012;20:1484-99.

13. Mengshol JA, Vincenti MP, Coon CI, Barchowsky A, Brinckerhoff CE. Interleukin-1 induction of collagenase 3 (matrix metalloproteinase 13) gene expression in chondrocytes requires p38, c-Jun N-terminal kinase, and nuclear factor kappaB: differential regulation of collagenase 1 and collagenase 3. Arthritis Rheum. 2000;43:801-11.

14. Choudhary N, Bhatt LK, Prabhavalkar KS. Experimental animal models for rheumatoid arthritis [review]. Immunopharmacol Immunotoxicol. 2018;40:193-200.

15. Caplazi P, Baca M, Barck K, Carano RA, DeVoss J, Lee WP, et al. Mouse models of rheumatoid arthritis [review]. Vet Pathol. 2015;52:819-26.

16. el-Deiry WS, Tokino T, Velculescu VE, Levy DB, Parsons R, Trent JM, et al. WAF1, a potential mediator of p53 tumor suppression. Cell. 1993;75:817-25.

17. Gu Y, Turck CW, Morgan DO. Inhibition of CDK2 activity in vivo by an associated 20K regulatory subunit. Nature. 1993;366:707-10.

18. Harper JW, Adami GR, Wei N, Keyomarsi K, Elledge SJ. The p21 Cdk-interacting protein Cip1 is a potent inhibitor of G1 cyclin-dependent kinases. Cell. 1993;75:805-16.

19. Xiong Y, Hannon GJ, Zhang H, Casso D, Kobayashi R, Beach D. p21 is a universal inhibitor of cyclin kinases. Nature. 1993;366:701-4.

20. Bedelbaeva K, Snyder A, Gourevitch D, Clark L, Zhang XM, Leferovich J, et al. Lack of p21 expression links cell cycle control and appendage regeneration in mice. Proc Natl Acad Sci USA. 2010;107:5845-50.

21. Olive M, Mellad JA, Beltran LE, Ma M, Cimato T, Noguchi AC, et al. p21Cip1 modulates arterial wound repair through the stromal cell-derived factor-1/CXCR4 axis in mice. J Clin Invest. 2008;118:2050-61.

22. Suzuki A, Tsutomi Y, Akahane K, Araki T, Miura M. Resistance to Fas-mediated apoptosis: activation of caspase 3 is regulated by cell cycle regulator p21WAF1 and IAP gene family ILP. Oncogene. 1998;17:931-9.

23. Seoane J, Le HV, Massagué J. Myc suppression of the p21 (Cip1) Cdk inhibitor influences the outcome of the p53 response to DNA damage. Nature. 2002;419:729-34.

24. Chinzei N, Hayashi S, Ueha T, Fujishiro T, Kanzaki N, Hashimoto S, et al. P21 deficiency delays regeneration of skeletal muscular tissue. PloS One. 2015;10:e0125765.

25. Deng C, Zhang P, Harper JW, Elledge SJ, Leder P. Mice lacking p21CIP1/WAF1 undergo normal development, but are defective in G1 checkpoint control. Cell. 1995;82:675-84.

26. Missero C, Di Cunto F, Kiyokawa H, Koff A, Dotto GP. The absence of p21Cip1/WAF1 alters keratinocyte growth and differentiation and promotes ras-tumor progression. Genes Dev. 1996;10:3065-75.

27. Hayashi S, Fujishiro T, Hashimoto S, Kanzaki N, Chinzei N, Kihara S, et al. p21 deficiency is susceptible to osteoarthritis through STAT3 phosphorylation. Arthritis Res Ther. 2015;17:314.

28. Kihara S, Hayashi S, Hashimoto S, Kanzaki N, Takayama K, Matsumoto T, et al. Cyclin-dependent kinase inhibitor-1-deficient mice are susceptible to osteoarthritis associated with enhanced inflammation. J Bone Miner Res. 2017;33:2242.

29. Mavers M, Cuda CM, Misharin AV, Gierut AK, Agrawal H, Weber E, et al. Cyclin-dependent kinase inhibitor p21, via its C-terminal domain, is essential for resolution of murine inflammatory arthritis. Arthritis Rheum. 2012;64:141-52.

30. Nonomura Y, Kohsaka H, Nagasaka K, Miyasaka N. Gene transfer of a cell cycle modulator exerts anti-inflammatory effects in the treatment of arthritis. J Immunol. 2003;171:4913-9.

31. Perlman H, Bradley K, Liu H, Cole S, Shamiyeh E, Smith RC, et al. IL-6 and matrix metalloproteinase-1 are regulated by the cyclin-dependent kinase inhibitor p21 in synovial fibroblasts. J Immunol. 2003;170:838-45.

32. Brand DD, Latham KA, Rosloniec EF. Collagen-induced arthritis. Nat Protoc. 2007;2:1269-75.

33. Glasson SS, Chambers MG, Van Den Berg WB, Little CB. The OARSI histopathology initiative - recommendations for histological assessments of osteoarthritis in the mouse. Osteoarthritis Cartilage. 2010;18 Suppl 3:S17-23.

34. Kraus VB, Huebner JL, DeGroot J, Bendele A. The OARSI histopathology initiative - recommendations for histological assessments of osteoarthritis in the guinea pig. Osteoarthritis Cartilage. 2010;18 Suppl 3:S35-52.

35. Yamada J, Tsuji K, Miyatake K, Matsukura Y, Abula K, Inoue M, et al. Follistatin alleviates synovitis and articular cartilage degeneration induced by carrageenan. Int J Inflam. 2014;2014:959271.

36. Arnett FC, Edworthy SM, Bloch DA, McShane DJ, Fries JF, Cooper NS, et al. The American Rheumatism Association 1987 revised criteria for the classification of rheumatoid arthritis. Arthritis Rheum. 1988;31:315-24.

37. Tsubosaka M, Kihara S, Hayashi S, Nagata J, Kuwahara T, Fujita M, et al. Gelatin hydrogels with eicosapentaenoic acid can prevent osteoarthritis progression in vivo in a mouse model. J Orthop Res. 2020;1– 13.

38. Fukumitsu S, Villareal MO, Fujitsuka T, Aida K, Isoda H. Anti-inflammatory and anti-arthritic effects of pentacyclic triterpenoids maslinic acid through NF-κB inactivation. Mol Nut Food Res. 2016;60:399-409.

39. Scatizzi JC, Mavers M, Hutcheson J, Young B, Shi B, Pope RM, et al. The CDK domain of p21 is a suppressor of IL-1beta-mediated inflammation in activated macrophages. Eur J Immunol. 2009;39:820-5.

40. Fujiwara N, Kobayashi K. Macrophages in inflammation [review]. Curr Drug Targets Inflamm Allergy. 2005;4:281-6.

41. Trakala M, Arias CF, Garcia MI, Moreno-Ortiz MC, Tsilingiri K, Fernandez PJ, et al. Regulation of macrophage activation and septic shock susceptibility via p21(WAF1/CIP1). Eur J Immunol.

2009;39:810-9.

42. Cheng CY, Kuo CT, Lin CC, Hsieh HL, Yang CM. IL-1beta induces expression of matrix metalloproteinase-9 and cell migration via a c-Src-dependent, growth factor receptor transactivation in A549 cells. Br J Pharmacol. 2010;160:1595-610.

43. Ghosh S, Karin M. Missing pieces in the NF-kappaB puzzle. Cell. 2002;109 Suppl:S81-96.

44. Fujikawa Y, Shingu M, Torisu T, Masumi S. Interleukin-1 receptor antagonist production in cultured synovial cells from patients with rheumatoid arthritis and osteoarthritis. Ann Rheum Dis. 1995;54:318-20.

45. Alsalameh S, Amin RJ, Kunisch E, Jasin H, Kinne RW. Preferential induction of prodestructive matrix metalloproteinase-1 and pro-inflammatory interleukin 6 and prostaglandin E2 in rheumatoid arthritis synovial fibroblasts via tumor necrosis factor receptor-55. J Rheumatol. 2003;30:1680-90.

46. Jiao Z, Wang W, Ma J, Wang S, Su Z, Xu H-X. Notch signaling mediates TNF-α-induced IL-6 production in cultured fibroblast-like synoviocytes from rheumatoid arthritis. Clin Dev Immunol. 2012;2012:350209.
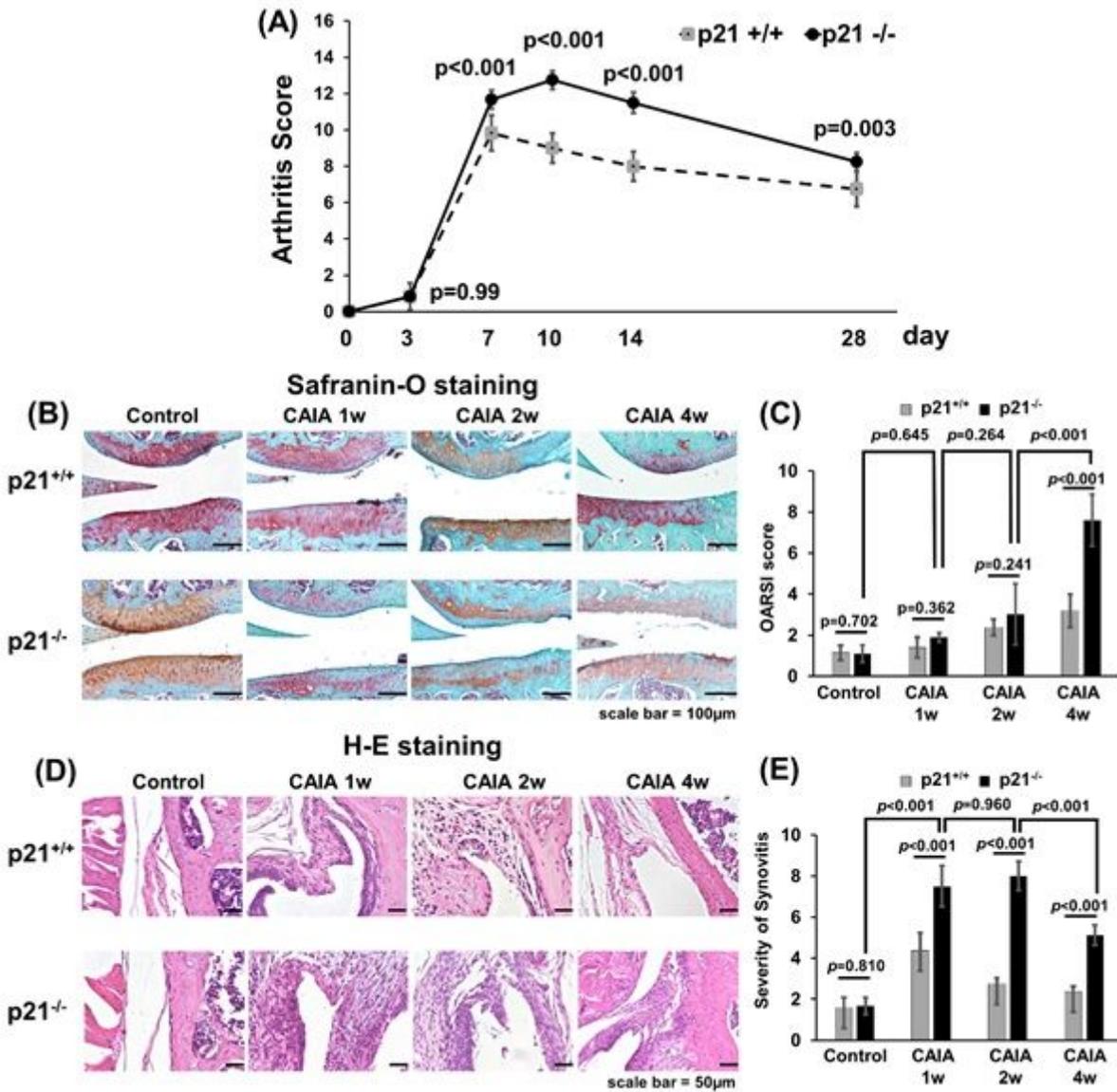
Figures

Figure 1

p21-deficient mice exhibit increased and prolonged inflammatory arthritis. (A) OARSI-based arthritis scores of p21-/- and p21+/+ mice on days 7, 10, 14, and 28 after administration of the antibody cocktail. Cartilage and synovial tissue samples were collected from the knee and stained with (B) Safranin-O and Fast Green, and (D) Hematoxylin and Eosin, respectively. (B, D) p21+/+ mice and p21-/- mice as controls and on days 7, 14, and 28. (C) Average sum of the OARSI cartilage OA-histopathology scores and (E) average severity of synovitis scores with 95% CI from four quadrants (i.e., medial femoral condyle, medial tibial plateau, lateral femoral condyle, and lateral tibial plateau) and eight sections per knee. Four mice were analyzed from each group. CI: confidence interval; CAIA: collagen antibody-induced arthritis; p21: cyclin-dependent kinase inhibitor 1.
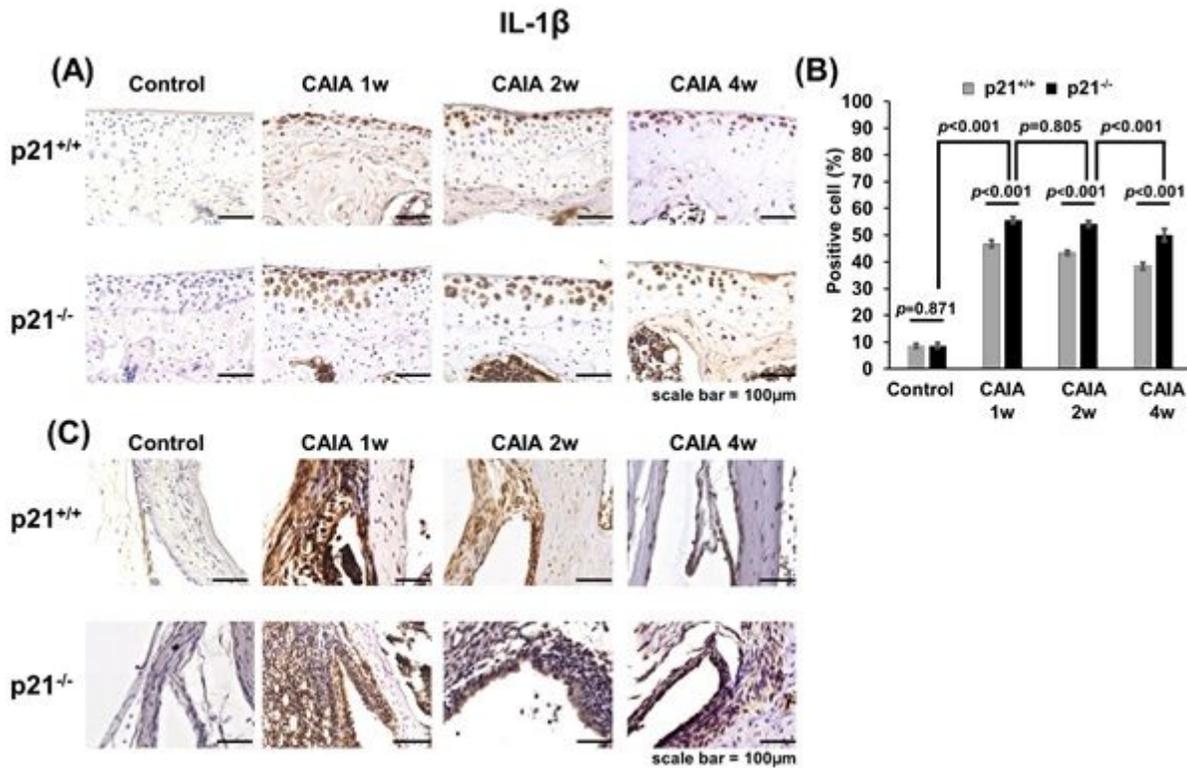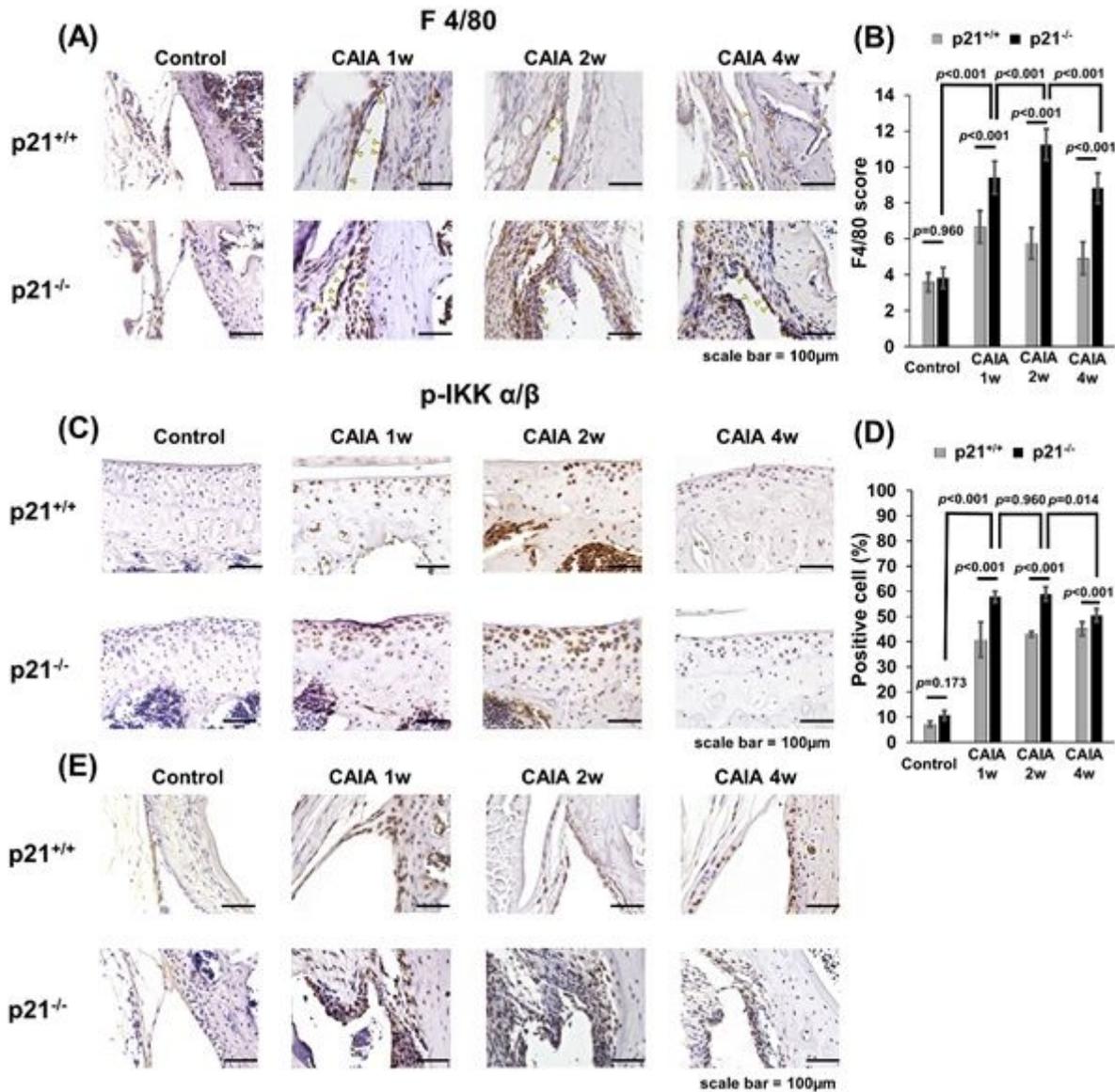
Figure 2

p21 levels influence the number of IL-1β-positive cells in the CAIA mouse model. (A) Cartilage and (C) synovial tissue samples were collected from the knees of mice after antibody cocktail administration. (A, C) p21+/+ mice and p21-/- mice as control and on days 7, 14, and 28. (B) The percentage of IL-1β-stained cells (number of positive cells/total number of cells) with 95% CI. The sections were counterstained with hematoxylin. Four mice were analyzed from each group. CI: confidence interval; CAIA: collagen antibody-induced arthritis; p21: cyclin-dependent kinase inhibitor 1.

Figure 3

p21 levels influence the number of F4/80- and p-IKKα/β-positive cells in the CAIA mouse model. (A, E) Cartilage and (C) synovial tissue samples were collected from the knees of mice after antibody cocktail administration. (A, C, E) p21+/+ mice and p21-/- mice as control and on days 7, 14, and 28. (B) Semiquantitative analysis of the infiltration of F4/80-positive cells into the synovial membrane. The average F4/80 score with 95% CI was calculated from all four quadrants. (D) The percentage of p-IKKα/β-stained cells (number of positive cells/ total number of cells) with 95% CI. The sections were counterstained with hematoxylin. Four mice were analyzed from each group. CI: confidence interval; IKK: IκB kinase complex; CAIA: collagen antibody-induced arthritis; p21: cyclin-dependent kinase inhibitor 1.
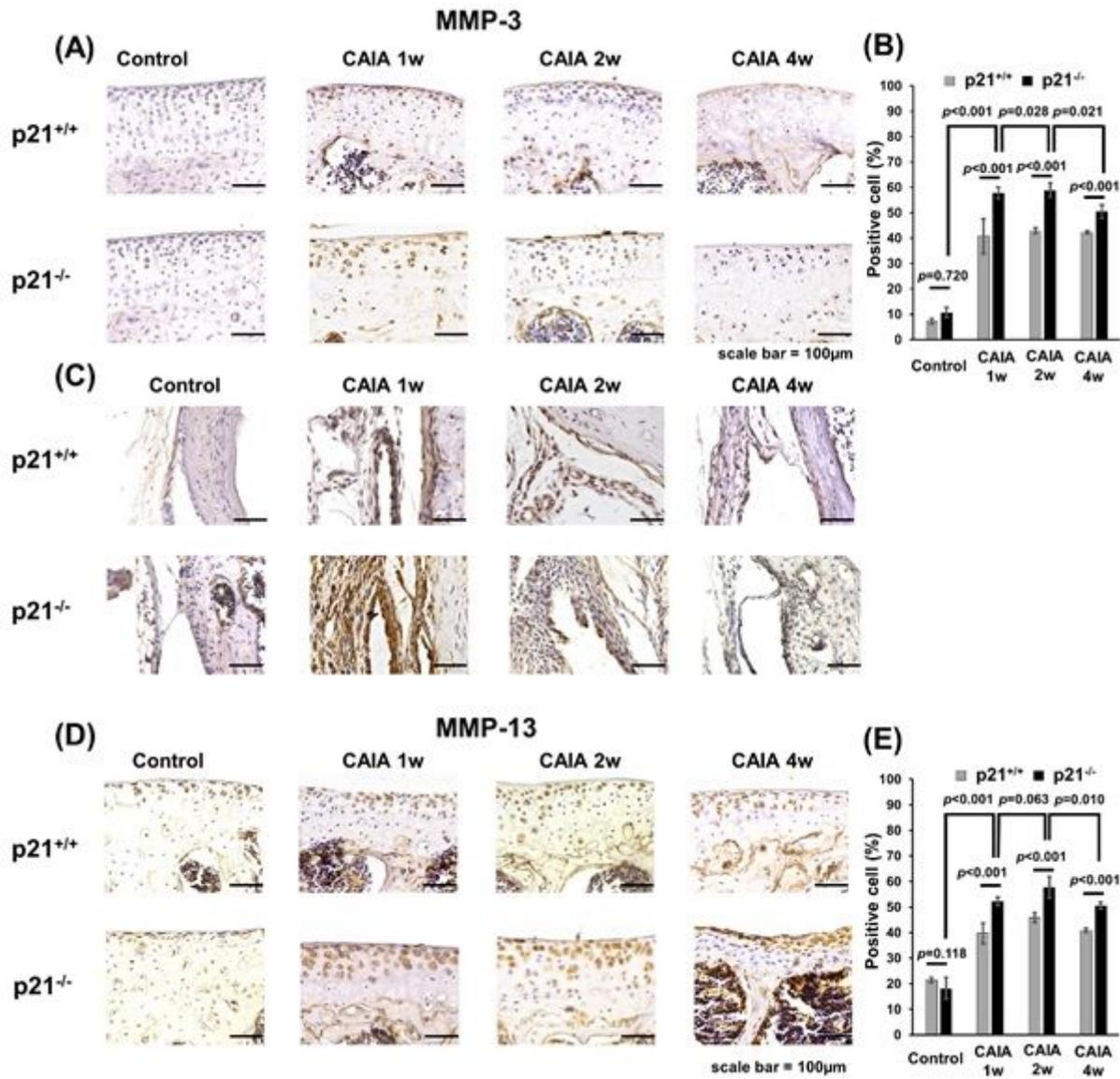
Figure 4

p21 levels influence the numbers of MMP-3- and MMP-13-positive cells in the CAIA mouse model. (A, D) Cartilage and (C) synovial tissue samples were collected from the knees of mice after antibody cocktail administration. (A, C, D) p21+/+ mice and p21-/- mice as control and on days 7, 14, and 28. (B) The percentage of MMP-3-stained cells (number of positive cells/total number of cells) with 95% CI. (E) The percentage of MMP-13-stained cells with 95% CI. The sections were counterstained with hematoxylin. Four mice were analyzed from each group. CI: confidence interval; CAIA: collagen antibody-induced arthritis; p21: cyclin-dependent kinase inhibitor 1.
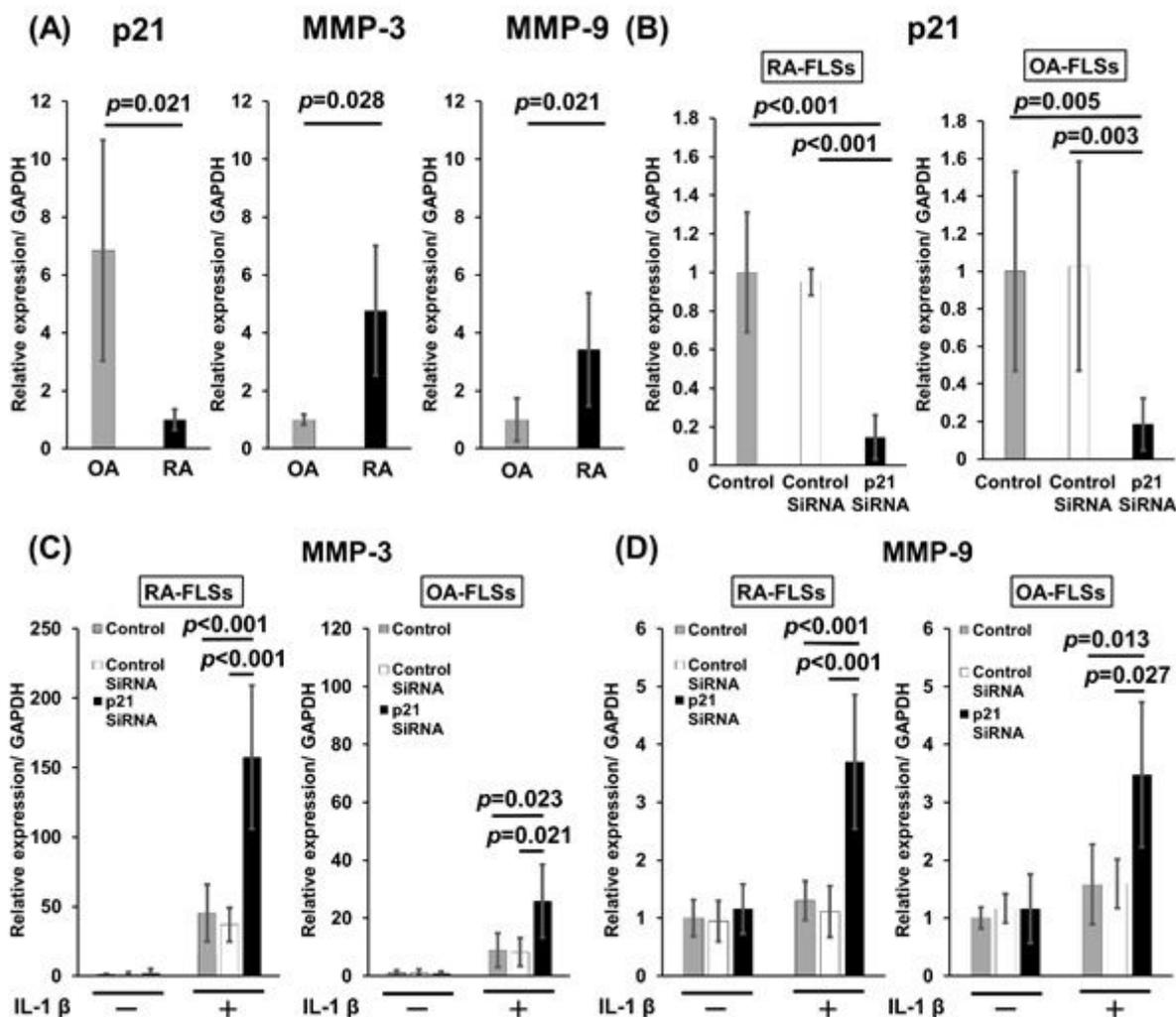
Figure 5

Downregulation of the p21 gene affects MMP expression in rheumatoid arthritis and osteoarthritis synovial tissues. (A) The relative expression of p21, MMP-3, and MMP-9 mRNA was determined in fibroblast-like synoviocytes (FLSs). (B) FLSs were transfected with p21 siRNA or nonspecific control siRNA for 24 h, and the relative expression of p21 mRNA was determined. The relative expression of (C) MMP-3 and (D) MMP-9 mRNA was determined after transfection with p21 siRNA or nonspecific control siRNA and treatment with or without 10 ng/ml recombinant human IL-1β for 24 h. The relative expression of MMP-3 and MMP-9 mRNA with respect to the control is shown with 95% CI. Five human synovial tissues were analyzed for each group.CI: confidence interval; FLSs: fibroblast like synoviocytes; p21: cyclin-dependent kinase inhibitor 1.
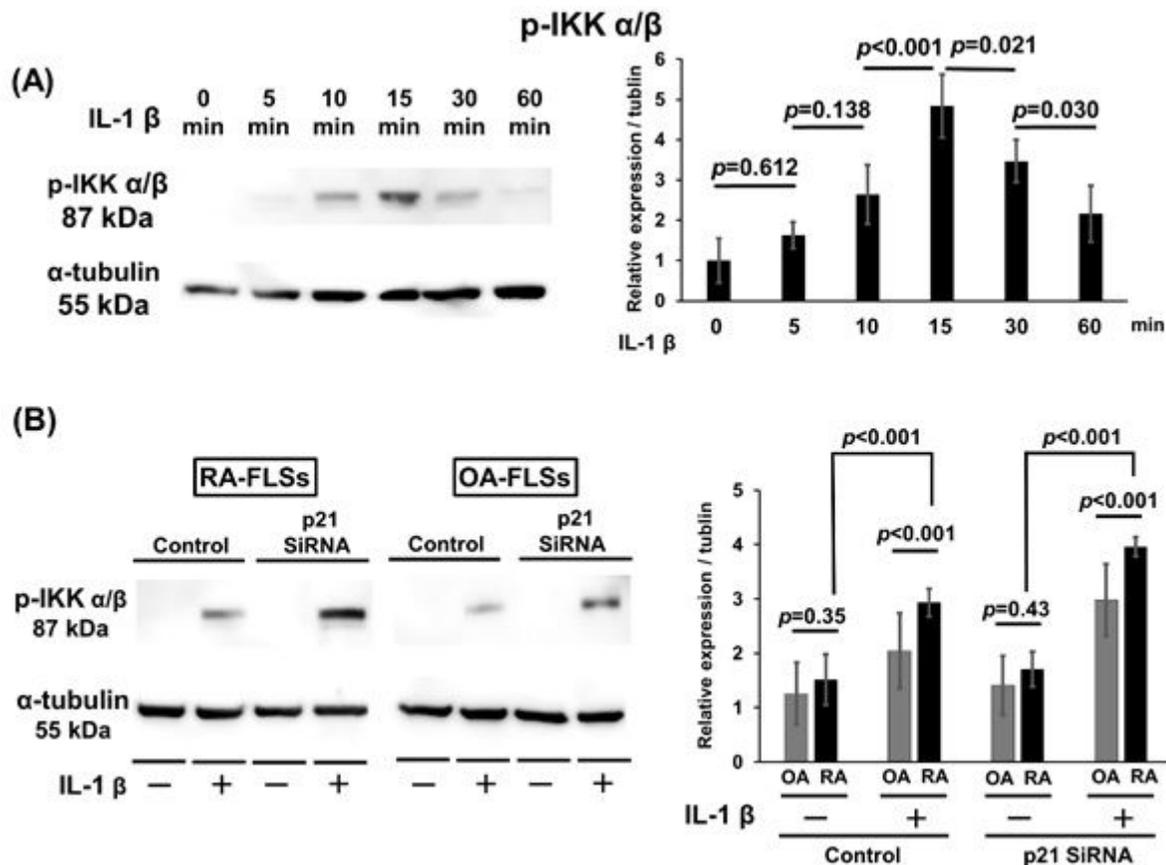
Figure 6

Downregulation of the p21 gene affects IKKα/β phosphorylation in rheumatoid arthritis synovial tissues. Western blotting was performed to analyze the (A) time-dependent IL-1β-induced phosphorylation of IKKα/β and (B) p-IKKα/β expression in RA and OA synovial cells after treatment with IL-1β for 15 min. (A, B) Expression was determined by semiquantitative analysis of digitally captured images. CI: confidence interval; FLSs: fibroblast like synoviocytes; IKK: IκB kinase complex; p21: cyclin-dependent kinase inhibitor 1.

Supplementary Files

This is a list of supplementary files associated with this preprint. Click to download.

- SupplementaryMaterial.docx